Model Calculations of Isotope Effects Using Structures Containing Low-Barrier Hydrogen Bonds

W. Phillip Huskey

Contribution from the Department of Chemistry (Newark Campus), Rutgers, The State University of New Jersey, Newark, New Jersey 07102

Received August 24, 1995[⊗]

Abstract: Isotope effect calculations (H/D and $^{16}O/^{18}O$) were carried out for a series of vibrational models containing a double-minimum potential for a hydrogen bond. The calculations showed the maximum hydrogen isotope effects for models in which the zero-point vibrational levels (for H) for the motion governed by the double-minimum potential were very near the energy of the barrier for the potential. The hydrogen isotope effects also showed a strong dependence on the energy difference between the wells of the double-minimum potential. Isotopic entropies were calculated for the H/D isotope effects, and were found to be dependent on the height of the barrier in the potential. Oxygen isotope effects were all inverse for reasons having little to do with the presence of double-minimum potentials in the models. The results have implications for studies of low-barrier hydrogen bonds.

Short, low-barrier hydrogen bonds[1,2] have been proposed recently to be important in enzymic catalysis,[2−4] although the scope of the role they play has been debated.[5] Outside of the current debate about enzymic catalysis, strong hydrogen bonds have long been considered as possible features of transition states for acid- and base-catalyzed reactions. Catalytic protons in transition states for certain reactions have been proposed to lie in stable hydrogen bond potentials, in part to help explain observations of small (near unity) kinetic isotope effects.[6] The notion of catalytic protons in stable potentials was later extended to include cases with larger kinetic isotope effects (ca. 2−4).[7] Kreevoy and Liang's[1] measurement of low isotopic fractionation factors for hydrogen-bonded bis-carboxylate complexes in a nonaqueous solvent helped to strengthen this conjecture. Kreevoy and Liang used the zero-point vibrational levels of model double-minimum potentials to explain their experimental findings. Hydrogen bonds of the type studied by Kreevoy and Liang are now called "low-barrier" hydrogen bonds.

A potential like the one shown in Figure 1 is commonly used to present the concept of a low-barrier hydrogen bond; it also serves here to define the barrier height ($V_{barrier}$) and the energy difference between the minima (ΔV_{min}). The curve for the potential plotted is a convenient quartic equation, eq 1, in which

$$2V = f_2x^2 + f_3x^3 + f_4x^4 \quad (1)$$

the coordinate x represents the displacement of the proton of the hydrogen bond along the heteroatom axis of the bond.[8] In the work presented here, x is the displacement of the asymmetric stretch of the hydrogen bond. When the parameters of the potential are set such that the barrier for proton motion along the hydrogen bond is low, and the distance between minima is small, the energy of the lowest vibrational state will approach that of the barrier height and the proton becomes highly delocalized.

Much of the recent discussion concerning the detection and characterization of low-barrier hydrogen bonds has focused on the use of NMR chemical shifts.[2,9] Studies of isotopic fractionation factors for hydrogen bonds[10] and the use of kinetic isotope effects may prove to be equally useful for sorting out the details of the potential defining the hydrogen bonds, especially for catalytically important bonds that should be found in transition-state structures. To aid in this effort, a method for building vibrational models for structures containing low-barrier hydrogen bonds, along with calculations for a model reaction, are presented here. These models will refer to low-barrier hydrogen bonds that exist in a transition state but are not coupled to the reaction-coordinate motion. Thus equilibrium isotope effects or fractionation factors can be used to describe kinetic isotope-effect contributions arising from the presence of low-barrier hydrogen bonds in the transition state.

[⊗] Abstract published in *Advance ACS Abstracts,* January 15, 1996.

(1) (a) Kreevoy, M. M.; Liang, T. M.; Chang, K. C. *J. Am. Chem. Soc.* **1977**, *99*, 5207−5209. (b) Kreevoy, M. M.; Liang, T. M. *J. Am. Chem. Soc.* **1980**, *102*, 3315−3322.

(2) Hibbert, F.; Emsley, J. *Adv. Phys. Org. Chem.* **1990**, *26*, 255−379.

(3) Cleland, W. W. *Biochemistry* **1992**, *31*, 317−319.

(4) Kreevoy, M. M.; Cleland, W. W. *Science* **1994**, *264*, 1887−1890.

(5) Scheiner, S.; Kar, T. *J. Am. Chem. Soc.* **1995**, *117*, 6970−6975. Warshel, A.; Papazyan, A.; Kollman, P. A. *Science* **1995**, *269*, 102−103. Cleland, W. W.; Kreevoy, M. M. *Science* **1995**, *269*, 104. Frey, P. A. *Science* **1995**, *269*, 104−106.

(6) Swain, C. G.; Kuhn, D. A.; Schowen, R. L. *J. Am. Chem. Soc.* **1965**, *87*, 1553−1561. Cordes, E. H. *Prog. Phys. Org. Chem.* **1967**, *4*, 1−44. Schowen, R. L. *Prog. Phys. Org. Chem.* **1972**, *9*, 275−331.

(7) Minor, S. S.; Schowen, R. L. *J. Am. Chem. Soc.* **1973**, *95*, 2279−2281. Young, P. R.; Jencks, W. P. *J. Am. Chem. Soc.* **1978**, *100*, 1228−1235. Eliason, R.; Kreevoy, M. M. *J. Am. Chem. Soc.* **1978**, *100*, 7037−7041. Hegazi, M.; Mata-Segreda, J. F.; Schowen, R. L. *J. Org. Chem.* **1980**, *45*, 307−310. Schowen, R. L. *Mol. Struct. Energ.* **1988**, *9*, 119−168 (Mechanistic Principles of Enzyme Activity; Liebman, J. F., Greenberg, A., Eds.). Gandour, R. D.; Nabulsi, N. A. R.; Fonczek, F. R. *J. Am. Chem. Soc.* **1990**, *112*, 7817−7819.

(8) Note that 1 mdyn·Å is equivalent to an energy of 10^{-18} J or 50 341 cm^{-1}.

(9) Perrin, C. L. *Science* **1994**, *266*, 1665−1668. Perrin, C. L.; Thoburn, J. D. *J. Am. Chem. Soc.* **1992**, *114*, 8559−8565. Perrin, C. L.; Thoburn, J. D. *J. Am. Chem. Soc.* **1989**, *111*, 8010−8012. Frey, P. A.; Whitt, S. A.; Tobin, J. B. *Science* **1994**, *264*, 1927−1930. Golubev, N. S.; Smirnov, S. N.; Gindin, V. A.; Denisov, G. S.; Benedict, H.; Limbach, H.-H. *J. Am. Chem. Soc.* **1994**, *116*, 12055−12056. Tong, H.; Davis, L. *Biochemistry* **1995**, *34*, 3362−3367. Tobin, J. B.; Whitt, S. A.; Cassidy, C. S.; Frey, P. A. *Biochemistry* **1995**, *34*, 6919−6924.

(10) Emsley, J.; Gold, V.; Szeto, W. T. A. *J. Chem. Soc., Dalton Trans.* **1986**, 2641−2644. Hibdon, S. A.; Coleman, C. A.; Wang, J.; Murray, C. J. *Bioorg. Chem.* **1992**, *20*, 334−344. Loh, S.; Markley, J. L. *Biochemistry* **1994**, *33*, 1029−1036. Arrowsmith, C. H.; Guo, H. X.; Kresge, A. J. *J. Am. Chem. Soc.* **1994**, *116*, 8890−8894. Kresge, A. J.; More O'Ferrall, R. A.; Powel, M. F. In *Isotopes in Organic Chemistry*; Buncel, E., Lee, C. C., Eds.; Elsevier: Amsterdam, 1987; Vol. 7, Chapter 4.

0002-7863/96/1518-1663$12.00/0

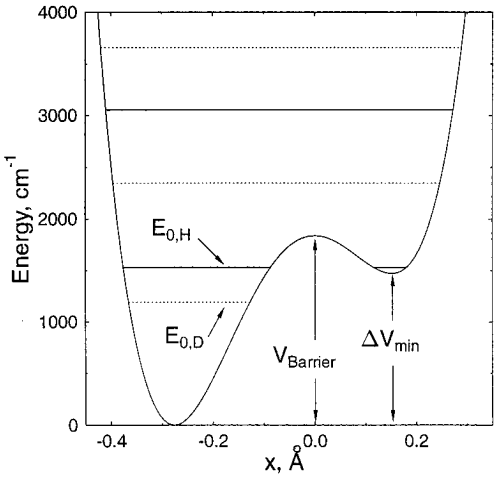

Figure 1. Description of terms used to define the double-minimum potentials. The potential (eq 1) shown is for $f_4 = 18$, $f_3 = 3$, $f_2 = -1.502$ (mdyn and Å units). The energy levels are for masses obtained using the method described in the text. In this case, for the H isotopomer the reduced mass for the coordinate is 0.4903 amu, and for the D isotopomer it is 0.9514 amu. Solid and dotted horizontal lines mark respective H and D vibrational energy levels for the potential.

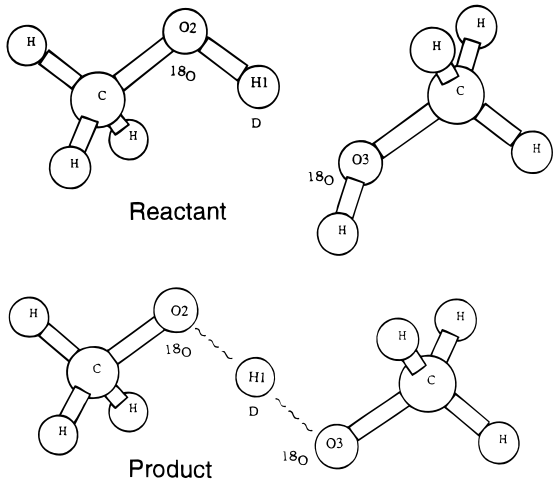

Figure 2. Models used for calculations of isotope effects. The positions of isotopic substitution are noted in the figure. All C−H (1.10 Å, 4.70 mdyn/Å) and C−O (1.43 Å, 4.30 mdyn/Å) bond lengths and stretching force constants were the same in the reactant and product models. All bond angles were fixed at tetrahedral values in the reactant and product, except for the linear O2−H1−O3 angle. The H−C−H bending force constant (0.50 mdyn·Å/rad^2) and the H−C−O force constant (0.85 mdyn·Å/rad^2) were also unchanged between the reactant and product models. The H−O−C bending force constants were 0.75 mdyn·Å/rad^2 in the reactant, and half this value in the product. Three redundant 4-atom chain torsional force constants were used for each of the C−O torsional coordinates. In the reactant, these values were 0.00833 mdyn·Å/rad^2, and half this value in the product. The H1−O3 stretching force constant was set to zero in the reactant, as were the O2−H1−O3 linear bending force constants in the product. The H1−O2 and H−O3 stretching constants were 6.838 mdyn/Å in the reactant. The O2−O3 distance was fixed between reactant and product as determined by the parameters of the double-minimum hydrogen bond potential in the product (see text). The treatment of the O−H coordinates in the product is described in the text.

Computational Methods

Isotope effects were calculated using a modification of the standard Bigeleisen−Wolfsberg[11] method in which classical partition functions are used to compute the contributions from translational and rotational degrees of freedom and vibrational contributions are computed using harmonic-oscillator partition functions for all vibrational degrees of freedom. The standard treatment was modified by replacing the harmonic vibrational term for asymmetric stretch involving dominant motions from atoms O2−H1−O3 in the product model with a partition function computed for a double-minimum potential.[12]

The general approach to the calculations was to first build reactant and product harmonic vibrational models (see Figure 2) using established procedures.[13] The product model at this stage represented the point at the top of the barrier for a double-minimum potential with one imaginary frequency corresponding to the motion across the barrier. In the second stage of the calculation, a vibrational partition function for the double minimum potential was used in place of what would be a term for the imaginary-frequency motion. The link between the harmonic vibrational analysis and the anharmonic analysis used for the double-minimum potential was the effective mass for the O2−H1−O3 asymmetric stretching motion.

Harmonic Vibrational Models. Most of the geometry and force constants for the reactant and product models are shown in Figure 1. Fully redundant simple valence harmonic force fields were designed for the reactant and product models based on force fields derived from normal-coordinate analyses of methanol spectra.[14] The O2−H1−O3 stretching force constants and bond distances were chosen based on the double-minimum parameters (f_2, f_3, and f_4) selected for a particular calculation. The O2−O3 distance was computed from eq 2, where

$$r_{O2-O3} = \Delta x + 2r^{o}_{O-H} \quad (2)$$

r^{o}_{O-H} is the bond length used for a unit bond order O−H bond (1.10 Å), and Δx is the distance between the minima of a double-minimum potential. For all calculations, once a distance for O2−O3 was determined from the double-minimum potential parameters for a product model, the same O2−O3 distance was used for the reactant. This was done primarily to minimize the size of rotational and translational contributions to the isotope effects. The O−H distances in the product were calculated from eq 3, in which $\Delta x'$ is the distance from $x = 0$

$$r_{O-H} = \Delta x' + r^{o}_{O-H} \quad (3)$$

(see Figure 1) to one of the minima of the potential. Stretching force constants for the O−H coordinates of the product were assigned using bond orders derived from the distance in eq 3, and a Badger's-rule[15] relationship (eqs 4 and 5). F^{o}_{O-H} is the force constant for a unit bond order O−H bond, and was assigned a value of 6.838 mdyn/Å to generate reactant model O−H stretching frequencies of 3500 cm^{-1}, the value used by Kreevoy and Liang[1b] for their reference model.

$$n_{O-H} = e^{\{(r^{o}_{O-H} - r_{O-H})/0.3\}} \quad (4)$$

(11) Bigeleisen, J.; Goeppert-Mayer, M. *J. Chem. Phys.* **1947**, *15*, 261−267. Wolfsberg, M.; Stern, M. J. *Pure Appl. Chem.* **1964**, *8*, 225−242.

(12) Several procedures could be used to calculate of vibrational partition functions for polyatomic molecules with anharmonic potentials. (Some examples include: Bowman, J. M. *J. Chem. Phys.* **1978**, *68*, 608−610. Alvarez-Collado, J. R.; Buenker, R. J. *J. Comput. Chem.* **1992**, *13*, 135−141. Maessen, B.; Wolfsberg, M. *J. Chem. Phys.* **1984**, *80*, 4651−4662. Martin, J. M. L.; Francois, J. P.; Gijbels, R. *J. Chem. Phys.* **1992**, *96*, 7633−7645. Isaacson, A. D.; Truhlar, D. G. *J. Chem. Phys.* **1984**, *80*, 2888−2896. Topper, R. Q.; Zhang, Q.; Liu, Y. P.; Truhlar, D. G. *J. Chem. Phys.* **1993**, *98*, 4991−5005. Galloy, C.; Lorquet, J. C. *Chem. Phys. Lett.* **1982**, *93*, 26−30). The method used here assumes that the partition function for one normal-mode (and harmonic) vibration can be replaced with a partition function for a vibrational potential defined by eq 1.

(13) (a) Melander, L.; Saunders, W. H., Jr. *Reaction Rates of Isotopic Molecules*; Wiley: New York, 1980. (b) Sims, L. B.; Lewis, D. E. *Isotopes in Organic Chemistry*; Buncel, E., Lee, C. C., Eds.; Elsevier: New York, 1984; Vol. 6, pp 161−259. (c) Buddenbaum, W. E.; Shiner, V. J., Jr. In *Isotope Effects on Enzyme Catalyzed Reactions*; Cleland, W. W., O'Leary, M. H., Northrop, D. R., Eds.; University Park Press: Baltimore, 1977; pp 1−36. (d) Huskey, W. P. In *Enzyme Mechanism from Isotope Effects*; Cook, P. F., Ed.; CRC Press: Boca Raton, FL, 1991; Chapter 2.

(14) Timidei, A.; Zerbi, G. *Naturforschung* **1970**, *25*, 1729−1731. Serrallach, A.; Meyer, R.; Gunthard, H. H. *J. Mol. Spectrosc.* **1974**, *52*, 94−129.

(15) Badger, R. M. *J. Chem. Phys.* **1935**, *3*, 710−714.

$$F_{O-H} = F^{o}_{O-H} n_{O-H} \quad (5)$$

A single off-diagonal force constant was included in the product force field to couple the O−H stretches and generate an imaginary frequency with a magnitude corresponding to the curvature at the barrier top of a particular double-minimum potential. For the potential of eq 1, the curvature at the barrier top is simply f_2. If this is compared with a linear triatomic asymmetric stretching force constant,[16] a valence stretch−stretch coupling constant (F_{ss}) can be found (eq 6).

$$f_2 = 0.5(F_{O2-H1} + F_{O3-H1} - 2F_{ss}) \quad (6)$$

The procedures outlined above produce harmonic vibrational models for the product that are specified by the parameters of the double-minimum potential, and represent structures situated at the top of the barrier for the same potential. Normal-coordinate calculations were carried out to obtain frequencies using the Gwinn method,[17] and standard harmonic oscillator partition functions were computed using all non-zero frequencies except for the single imaginary frequency in the product. Partition functions for double-minimum (quartic) potentials were incorporated into the calculation as described below.

Vibrational Analysis for Quartic Potentials. Solutions to the one-dimensional, quartic-potential, vibrational problem were obtained using a variational method with harmonic-oscillator basis functions.[18] In all cases, the 20 basis functions used were more than sufficient for convergence of isotopic partition functions evaluated up to 373 K. The necessary integrals for the method are simple analytical equations.[19b] Vibrational partition functions were computed by summing the Boltzmann factors for the various energy levels (up to 10 000 cm^{-1}) obtained from the variational calculation. The masses used in the calculation of energy levels for the quartic potentials were obtained from the normal-coordinate treatment of the purely harmonic models.

Effective Masses from Normal-Coordinate Analysis. The effective mass for the motion in the double-minimum potential was obtained from the internal-coordinate eigenvector for the imaginary asymmetric stretch (O2−H1−O3) frequency. The determination of effective masses from normal-coordinate treatments can be demonstrated in general terms by noting that the eigenvector matrix[20] in internal coordinates (**L**) diagonalizes (eq 7) the internal-coordinate force-constant matrix (**F**).[19]

$$\mathbf{L}^T\mathbf{F}\mathbf{L} = \mathrm{diag}(4\pi^2\nu_k^2) \quad (7)$$

Thus for the kth normal coordinate, it is possible to write eq 8,

$$\mathbf{L}_k^T\mathbf{F}\mathbf{L}_k = 4\pi^2\nu_k^2 \quad (8)$$

where $\mathbf{L}_k$ is the eigenvector (in terms of internal coordinates) for the kth frequency. An analogy can be seen between the equation above (eq 8) and the equation below (eq 9) for a diatomic stretch, with $\mathbf{L}_k^T\mathbf{L}_k$

$$F/\mu = 4\pi^2\nu^2 \quad (9)$$

(the squared length of the eigenvector) as the functional equivalent of the inverse of the reduced mass (μ). The column of **L** corresponding to the motion desired for a double-minimum potential (in this case, the imaginary asymmetric-stretching frequency) was used (as $\mathbf{L}_k^T\mathbf{L}_k$) to establish an effective mass for the one-dimensional quartic vibrational problem described above.

All calculations were carried out using a program written locally (vibie2). A single isotope-effect calculation for the full model required only a few seconds of time on a Silicon Graphics, Inc. Indigo2 workstation.

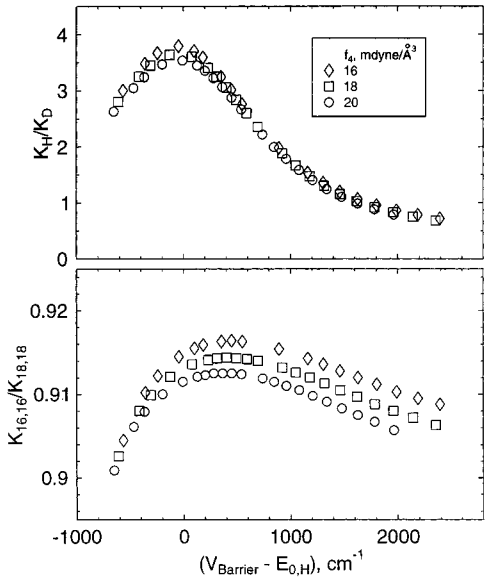

Figure 3. Isotope effects (25 °C) calculated for the model of Figure 2 displayed as a function of the difference between the double-minimum barrier height and the lowest H energy level for the double-minimum coordinate.

Results

Isotope effects calculated for the model described in Figure 2 are very sensitive to the height of the barrier within the hydrogen bond potential. Kreevoy and Liang[1b] found the same trend in hydrogen isotope effects in their simpler model which considered only the zero-point energy levels of double-minimum potentials. The results shown in the upper panel of Figure 3 demonstrate further that barrier height, when measured relative to the lowest energy level for the vibration, is a particularly good correlate of the hydrogen isotope effect. Calculations for models with a modest range of quartic constants (f_4, eq 1) are nearly superimposable. Similar results were found for the oxygen isotope effects (lower panel of Figure 3), but these values were more sensitive to the choice of f_4. Table 1 shows the contributions to the isotope effects from harmonic vibrational modes (HARM) and from the vibrational mode for the anharmonic double-minimum potential (DM) for a few points selected from Figure 3.

Isotopic entropy differences were also calculated for each of the points shown in Figure 1. Figure 4 shows the results for hydrogen isotope effects are, like the isotope effects, strongly correlated with the barrier height measured above the zero-point vibrational level. Isotopic entropies were obtained from the intercepts of linear plots of $\ln(K_H/K_D)$ vs $1/T$ for isotope effects calculated at 12 temperatures over a range of 273 to 373 K.

Figure 5 and Table 2 display results from a series of calculations in which the difference in the minima of the hydrogen bond potential was varied. Following the lead of Kreevoy and Liang,[1b] the cubic constant (f_3) of eq 1 was gradually increased to generate an appropriate set of models.

Discussion

The results of the calculations reported here have relevance to chemical and biochemical systems beyond the model's

(16) Hertzberg, G. *Molecular Spectra and Molecular Structure II. Infrared and Raman Spectra of Polyatomic Molecules*; D. Van Nostrand, Inc.: Princeton, NJ, 1945; p 172.

(17) Gwinn, W. D. *J. Chem. Phys.* **1971**, *55*, 477−481.

(18) Heilbronner, E.; Rtishauser, H.; Gerson, F. *Helv. Chim.* Acta **1959**, *42*, 2285−2303. Chan, S. I.; Stelman, D. *J. Mol. Spectrosc.* **1963**, *10*, 278−299. Chan, S. I.; Stelman, D.; Thompson, L. E. *J. Chem. Phys.* **1964**, *41*, 2828−2835.

(19) (a) Wilson, E. B., Jr.; Decius, J. C.; Cross, P. C. *Molecular Vibrations. The Theory of Infrared and Raman Vibrational Spectra*; McGraw-Hill Book Company: New York, 1955 (Dover edition, 1980). (b) Reference 19a, Appendix III.

(20) The Gwinn method[17] used for normal-coordinate analysis provides the eigenvectors in mass-weighted Cartesian coordinates. This matrix ($\mathbf{L}_{mc}$) was transformed into internal-coordinate eigenvectors using the **B** matrix (relating internal and Cartesian coordinates) already built for the Gwinn method ($\mathbf{L} = \mathbf{B}(\mathbf{M}\mathbf{L}_{mc})$, where **M** is a diagonal matrix containing inverse square roots of atomic masses).

Table 1. Isotope Effects as a Function of Barrier Height with $\Delta V_{min} = 0$[a] (See Figure 3)

f_2, mdyn/Å	$V_{barrier}$, cm^{-1}	$E_{0,H}$,[c] cm^{-1}	K_H/K_D (1st line), $K_{16,16}/K_{18,18}$ (2nd line)			
			MMI[b]	HARM[b]	DM[b]	IE[b]
−3.000	3146	1830	1.0004	10.8787	0.1197	1.3024
			0.9942	0.9269	0.9888	0.9113
−1.804	1138	1059	1.0002	10.5426	0.3416	3.6020
			0.9942	0.9251	0.9933	0.9136
−1.502	789	917	1.0001	10.4376	0.3484	3.6373
			0.9942	0.9245	0.9931	0.9121
−1.200	503	812	1.0000	10.3195	0.3338	3.4449
			0.9942	0.9219	0.9927	0.9099
-0.600	126	738	0.9999	10.0197	0.2799	2.8045
			0.9943	0.9153	0.9918	0.9026

[a] The quartic constant (f_4) for each of double-minimum potentials was set to 18 mdyn/Å^3, and the cubic constant (f_3) was zero. Calculations refer to the model in Figure 2 for 25 °C. [b] MMI is the usual contribution to the isotope effect (IE) arising from classical rotations and translations. HARM is the ratio of isotopic partition functions for all of the harmonic vibrational modes of the model (less the mode for the imaginary frequency corresponding to the H-bond asymmetric stretch). DM is the ratio of isotopic partition functions for vibrations of the double-minimum potential. [c] Lowest vibrational energy level for the double-minimum potential.

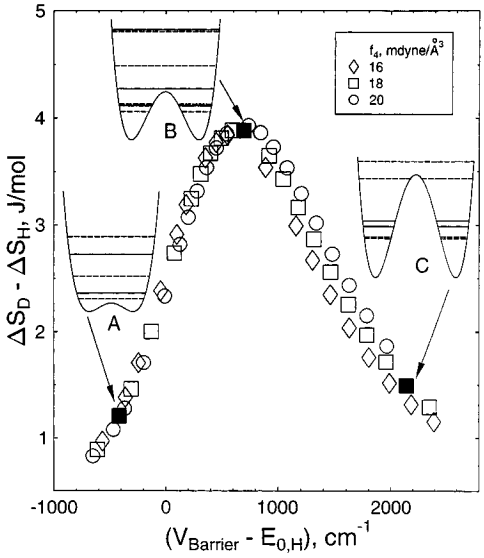

Figure 4. Isotopic entropy differences calculated for the model shown in Figure 2. Vibrational energy levels (solid = H, dashed = D) for three double-minimum potentials in the model are shown on the plot. The energy scale for each of the potentials plotted on the figure is 0−5000 cm^{-1}. The barrier heights (cm^{-1}) and f_2 (eq 1, mdyn/Å) for these potentials are the following: (A) 350, −1.00; (B) 2014, −2.40; and (C) 4282, −3.50.

nominal representation of a methanol dimer and hypothetical complexes of methoxide and methanol. These structures were chosen because they have simple geometries and they are convenient for testing ideas about hydrogen and oxygen isotope effects. The models could be changed and the parameters adjusted to attempt better quantitative agreement with specific experimental results. The results also have implications for both equilibrium and rate studies. The model calculations here all represent an equilibrium situation between reactant and product states, but the hydrogen-bonded product complex could easily be envisioned as a model for part of a transition-state structure involving heavy-atom rearrangement along an authentic reaction coordinate with a stable hydrogen bond as one element of the structure.

Hydrogen Isotope Effects and Isotopic Entropies. The hydrogen isotope effects reported in Figure 3 show a maximum value of 3.8 at the point where the zero-point energy for the H

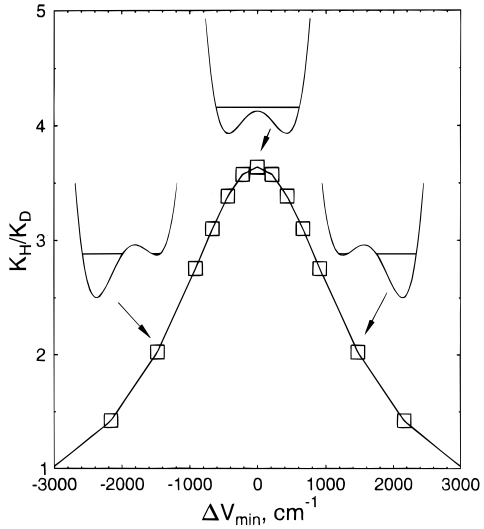

Figure 5. Hydrogen isotope effects (25 °C) as a function of the energy difference between the wells of a double-minimum potential for the model shown in Figure 1. The zero-point energies for the light isotopomer of the model are shown for three potentials. The energy scale for the plots of hydrogen bond potentials is 0−4000 cm^{-1}.

isotopomer equals the barrier height. As Table 1 shows, the variability in the isotope effect arises from changes in the vibrational levels corresponding to the double-minimum potential (DM in the table). For all of the product complexes in Figure 3 and in Table 1, the forces on either side of the hydrogen bond proton are balanced. The harmonic symmetric stretch of the hydrogen bond is therefore insensitive to the mass of the proton, so nearly complete loss of the reactant-state isotopic energy difference is seen in the harmonic contributions (HARM) to the isotope effect.[21] The effect of the double-minimum potential is to restore isotopic vibrational energy differences to the product complex. This effect is minimized, for the series of potentials examined here, when the zero-point level for H is near the barrier height. At this point, the H and D double-minimum vibrational levels become much closer in energy than would be expected for a harmonic potential. The same observations were also made by Kreevoy and Liang[1b] in their model calculations of isotopic fractionation factors.[22] The results of Figure 3 highlight the utility of isotope-effect measurements in learning about hydrogen bond potentials.

More refined models for hydrogen bond potentials could be developed in favorable cases where precise studies of the temperature dependence of isotope effects are possible. As Figure 4 shows, the isotopic entropy differences for the hydrogen isotope effects are also very sensitive to the barrier height, measured from the zero-point level of the hydrogen bond potential. The maximum in this plot occurs not at the point where the zero-point matches the barrier height, but instead for the potential shown at location B in the figure. At this point, the potential is such that the tunnel splitting of the lowest D level generates more low-lying vibrational states than for H. As can be seen from the potential at point B, there are four vibrational states below 5000 cm^{-1} for the deuterium isotopomer, but only three for the hydrogen isotopomer. In studies of kinetic isotope effects, it is common to use an isotopic Arrhenius equation to treat temperature effects,[13a] yielding isotope effects on pre-exponential parameters (A_H/A_D) and activation energies ($E_D - E_H$). The maximum isotopic entropy

(21) Westheimer, F. H. *Chem. Rev.* **1961**, *1*, 265−273. Bigeleisen, J. *Pure Appl. Chem.* **1964**, *8*, 217−233.

(22) The inverse of the isotopic fractionation factors calculated by Kreevoy and Liang[1b] is equivalent in kind to the K_H/K_D presented here.

Table 2. Isotope Effects for Models Containing Potentials with Varying ΔV_{min}[a] (See Figure 5)

f_3, mdyn/Å^2	$V_{barrier}$, cm^{-1}	$E_{0,H}$,[c] cm^{-1}	ΔV_{min}, cm^{-1}	K_H/K_D (1st line), $K_{16,16}/K_{18,18}$ (2nd line) MMI[b]	HARM[b]	DM[b]	IE[b]
0.0	789	917	0	1.0001	10.4376	0.3484	3.6373
	n_{OH} = 0.506, 0.506[d]			0.9942	0.9245	0.9931	0.9121
1.0	1040	1125	432	1.0001	10.4369	0.3244	3.3863
	n_{OH} = 0.488, 0.524			0.9942	0.9238	0.9928	0.9119
2.0	1380	1328	912	1.0001	10.4281	0.2640	2.7532
	n_{OH} = 0.434, 0.573			0.9942	0.9236	0.9923	0.9111
3.0	1838	1531	1472	1.0001	10.4173	0.1941	2.0224
	n_{OH} = 0.398, 0.604			0.9942	0.9232	0.9913	0.9099
4.0	2453	1731	2162	1.0001	10.4034	0.1365	1.4206
	n_{OH} = 0.363, 0.633			0.9942	0.9228	0.9902	0.9085

[a] Calculations are for the model in Figure 2 at 25 °C with f_4 = 18 mdyn/Å^3 and f_2 = −1.502 mdyn/Å. [b,c] Refer to footnotes of Table 1. [d] The two values listed for n_{OH} are the two O−H bond orders calculated using $e^{\{(1.1-r_{OH})/0.3\}}$ where r_{OH} is the bond length in Å as determined from the coordinates of the minima and maximum of the double-minimum potential.

difference in Figure 4 corresponds to an A_H/A_D value of 0.62. High-precision measurements of isotope effects would be needed to distinguish this modest deviation from a classical A_H/A_D value of near unity.[23]

Oxygen Isotope Effects. One of the motivations for devising a scheme for incorporation of double-minimum potentials into vibrational models was to learn about the possible utility of oxygen isotope effects in distinguishing among types of hydrogen bonds. Inspection of Table 1 reveals that the influence of the double-minimum potential on the isotope effects is small, but the changes that were observed as the barrier height was adjusted are similar to what was found for the hydrogen isotope effects. When the zero-point levels are near the barrier, the ^{16}O and ^{18}O energies tend to move closer together than would be expected in a harmonic potential. Coupled with studies of hydrogen isotope effect, studies of oxygen isotope effects could help define hydrogen bond potentials.

As Figure 3 and Table 1 show, the oxygen isotope effects are all inverse, and the largest component of the effect is the contribution from harmonic vibrations. The origin of the inverse nature of the isotope effect does not lie in the formation of a "tighter" potential in the product, but results instead from the new kinetic coupling of the product. As the complex is formed, high-frequency O−H stretches that are insensitive to the mass of oxygen are replaced by new low-frequency modes that resemble O−O stretching motions which are more sensitive to the mass of oxygen. The isotopic vibrational energy differences thus increase in the product complex and produce an inverse isotope effect. The oxygen isotope effects are inverse on these models even when there is no explicit force-field coupling present.

Influence of ΔV_{min} on Hydrogen Isotope Effects. The hydrogen isotope effects are sensitive to the energy difference between the minima of the hydrogen bond potential, as is seen in Figure 5 and Table 2. This result has implications for systems showing solvent isotope effects that are strongly dependent on the pK_a difference between reacting acids and bases.[24] For example, Bergman, Chiang, and Kresge[24a] found that the solvent isotope effect on the general-acid-catalyzed reaction between methoxylamine and *p*-methoxybenzaldehyde varied from 1.0 to 2.8 and back to near unit values over a pK_a range of 7 units for the general acid. The width at half-height of the peak in the solvent isotope effect is about 4 pK_a units. Yang and Jencks[24b] observed a similar peak in solvent isotope effects in plots against the pK_a's of the conjugate acids of general bases in the aminolysis of methyl formate with aniline. Fischer et al.[24c] also found similar results in the general-base-catalyzed hydroxyaminolysis of an iminium ion. Cox and Jencks[24d,e] observed a steeper dependence of solvent isotope effect on the pK_a of general acids in the reaction of methoxylamine with phenyl acetate. In this case, the width at half-height was only about 2 pK_a units. As was noted in each of these examples, the results were consistent with shifts in the rate-limiting step of the reaction which allowed the extent of rate control by a proton transfer step to vary as the pK_a of one reactant was varied. In one of the two models used to explain their results, Cox and Jencks[24e] found it necessary to force a strong pK_a dependence of the intrinsic isotope effect for the proton transfer step in a mechanism containing pK_a-sensitive rate-limiting steps.

The peak in the variation of isotope effects with ΔV_{min} in Figure 5 has a width at half-height of 2200 cm^{-1} which is equivalent to 4.6 pK_a units. Thus the "pK_a" dependence of the calculated isotope effects is not as steep as that seen by Cox and Jencks,[24d,e] but it is comparable to the other reports[24a−c] of pK_a-dependent solvent isotope effects. In light of the present calculations, the explanations used previously to explain maxima in solvent isotope effects still appear to be quite reasonable, but they could be augmented by allowing for the possibility of low-barrier hydrogen bonds in the transition states.

Over the range of product models giving this high variability in the isotope effect, there is only a modest change in the bond orders of the two O−H bonds.[25] As Table 2 shows, the bond orders are not far from 0.5 (0.36 and 0.63) when the isotope effect is 1.4. The bond orders in Table 2 are "effective" bond orders because they represent distances calculated using the coordinates for the minima and maxima of the double-mimimum potential.[26] As effective bond orders, they reflect measures of structure that might be determined from free-energy relationships. These computational results support a shifting, low-

(23) It is worth recalling that unusual temperature effects in kinetic isotope effect studies sometimes arise from temperature-induced changes in mechanism or changes in rate-limiting step or from reaction-coordinate tunneling. Complete elimination of these possible interpretations would be challenging.

(24) (a) Bergman, N. Å.; Chiang, Y.; Kresge, A. J. *J. Am. Chem. Soc.* **1978**, *100*, 5954−5956. (b) Yang, C. C.; Jencks, W. P. *J. Am. Chem. Soc.* **1988**, *110*, 2972−2973. (c) Fisher, H.; DeCandis, F. X.; Ogden, S. D.; Jencks, W. P. *J. Am. Chem. Soc.* **1980**, *102*, 1340−1347. (d) Cox, M. M.; Jencks, W. P. *J. Am. Chem. Soc.* **1978**, *100*, 5956−5957. (e) Cox, M. M.; Jencks, W. P. *J. Am. Chem. Soc.* **1981**, *103*, 572−580.

(25) Note that in Table 2, the variability in the isotope effect comes entirely from DM, the contributions from the vibrational energy levels of the double-minimum potential. The contributions from the harmonic vibrations are nearly constant. Part of this constancy comes from the fact that there is only a modest change in the O−H bond orders over the series of models used for the products. Another reason is the fact that high coupling constants were needed to generate harmonic vibrational models that matched the curvature at the barrier tops of double-minimum potentials (the imaginary frequencies ranged from 2284*i* to 3011*i* cm^{-1} for the calculations in Table 2). In the limit of high coupling, the stable symmetric stretch frequency, which governs the "Westheimer effect",[21] tends to become independent of the coupling strength and modest changes in structure.

barrier, hydrogen bond mechanism as an explantion for modest-sized kinetic isotope effects that are sensitive to pK_a, in situations where other indicators suggest modest variability in transition-state structure.

Conclusions

Knowledge about hydrogen-bond potentials in interesting chemical and biochemical systems could be advanced though careful measurements of isotope effects and their dependence on temperature. In ideal situations, experiments might be designed such that the pKa's of putative hydrogen-bond donor and acceptor groups could be systematically varied. In cases of greatest relevance to catalysis, namely systems with transition states bearing protonic bridges, kinetic isotope effects studies of this sort offer the most direct approach to characterizing the hydrogen-bond potential.

(26) If O−H and O−D bond distances are computed from the average position determined for the wave function of each vibrational level, weighted by the appropriate Boltzmann factor for 25 °C, a separate set of bond orders can be found for each of the model calculations in Table 2 when f_3 is nonzero. The results of this procedure are as follows: $f_3 = 1.0$ mdyn/Å^2, $n_{OH} = 0.565$ and 0.450, $n_{OD} = 0.624$ and 0.408; $f_3 = 2.0$, $n_{OH} = 0.627$ and 0.397, $n_{OD} = 0.729$ and 0.342; $f_3 = 3.0$, $n_{OH} = 0.697$ and 0.345, $n_{OD} = 0.802$ and 0.300; $f_3 = 4.0$, $n_{OH} = 0.761$ and 0.302, $n_{OD} = 0.851$ and 0.207.

Acknowledgment. Support from the Petroleum Research Fund, administered by the American Chemical Society, and from the Rutgers Research Council is gratefully acknowledged.

JA9529246